Computer Assisted Mechanics and Engineering Sciences, 4: 3–25, 1997.

The role of parallel computing in the stability analysis of aerospace shell structures

Johann Arbocz[†] and Jan Hol[‡]
Faculty of Aerospace Engineering, Delft University of Technology, The Netherlands

(Received May 27, 1996)

The development of "DISDECO", the **D**elft **I**nteractive **S**hell **DE**sign **CO**de is described. The purpose of this project is to make the accumulated theoretical, numerical and practical knowledge of the last 25 years or so readily accessible to users interested in the analysis of buckling sensitive structures. With this open ended, hierarchical, interactive computer code the user can access from his workstation successively programs of increasing complexity. The computational modules currently operational in DISDECO provide the prospective user with facilities to calculate the critical buckling loads of stiffened anisotropic shells under combined loading, to investigate the effects the various types of boundary conditions will have on the critical load, and to get a complete picture of the degrading effects the different shapes of possible initial imperfections might cause, all in one interactive session. Once a design is finalized, its collapse load can be verified by running a large refined model remotely from behind the workstation with one of the current generation 2-dimensional codes, with advanced capabilities to handle both geometric and material nonlinearities.

1. INTRODUCTION

In modern designs, which are often obtained by one of the structural optimization codes and which are made out of high strength materials (read advanced composites), it happens frequently that the stability behavior dictates the choice of some of the critical dimensions of the structures. This implies that one has to investigate the different loading cases quite accurately by carrying out extensive numerical calculations and/or experimental verifications.

Twenty five years ago it was so that numerical results were looked upon with a certain degree of distrust and they were only accepted if supported by some other facts. Now-a-days, as the older generation of engineers (the ones who have gotten their degrees before the advent of computers) is retiring and the younger ones with extensive training in the ever-so-popular finite element techniques take over, one begins to encounter in technical discussion a new mentality; the insight of how structures behave under loading of the older generation is being replaced more and more by the nearly religious faith of the younger ones in the predictions of their favorite computer codes.

Actually what one needs is not more of one and less of the other (and the reader is free to associate his preference with one or the other), but an optimal combination of both, namely insight into structural behavior and familiarity with the appropriate numerical techniques.

It has been demonstrated in the past [1] that reliable buckling load predictions for imperfection sensitive structures depend mainly on the availability of a sufficiently detailed statistical sample of the expected initial imperfections and on the appropriate choice of the nonlinear model used for the buckling load calculations. The latter, in turn, requires considerable knowledge by the user as to the physical behavior of imperfect shell structures. It is felt that this knowledge can best be acquired by first using the series of imperfection sensitivity analyses of increasing complexity that have been published in the literature [2, 3, 4].

[†] Professor of Aircraft Structures

[‡] Assistant Professor

To provide the means for such a refined computer supported design approach the development of DISDECO, the **D**elft **I**nteractive **S**hell **DE**sign **CO**de has been initiated. When finished this open ended, hierarchical, interactive computer code will provide for easy access to the theoretical knowledge and practical experience, that has been accumulated by the many scientists who have been active in the field of shell stability, via the advanced interactive and computational facilities offered by modern high-speed 64 bit personal workstations. Great care is being taken to present the results in a unified form so as to make it easy for the user to proceed step-by-step from the simpler approaches used by the early investigators to the more sophisticated analytical and numerical methods used presently.

Another purpose of the development of DISDECO is to provide a research tool for the systematic exploration of the different assumptions made when one estimates the buckling loads and mode shapes of imperfect anisotropic ring or stringer stiffened cylindrical shell subject to combined loading conditions.

When working with DISDECO a user, who is aware of the latest theoretical developments, can easily investigate the effects of using membrane or nonlinear prebuckling, of enforcing rigorously different combinations of boundary conditions at the shell edges, or he can estimate the degrading of the critical buckling load by the various initial imperfection shapes which can occur in practice.

For initial estimates one usually relies on the solutions of Donnell type equations. For more accurate analysis DISDECO contains also computational modules based on Flügge or Novozhilov type equations. The level of hierarchy is based on the complexity of the solution procedure used.

Thus the initial level consists of semi-analytical solutions for the buckling load of perfect, anisotropic circular cylindrical shells under axial compression, internal or external pressure, torsion and bending. Also included are modules that contain Koiter's imperfection sensitivity theory extended to anisotropic shell structures under combined loading.

The Level-2 solutions employ a truncated Fourier expansion in the circumferential direction and solve the resulting ordinary differential equations forming a nonlinear eigenvalue problem by a Stodola like technique. This involves the numerical integration of the set of ordinary differential equations, which in turn makes it possible to satisfy the specified boundary conditions rigorously.

Finally, the highest level of complexity can be provided by any of the currently available 2-dimensional finite element or finite difference codes which include advanced geometric and material nonlinearity capabilities. These codes can be brought via interfaces within the interactive, menu-prompted environment of DISDECO. Thus it is possible to use the same pre- and postprocessing facilities at all 3-levels of computational complexity.

2. Basic lay-out of DISDECO

As mentioned above the hardware component which plays a central role in the development of DISDECO is the modern, high-speed, 64 bit graphic workstation with its own external storage disk. Although most problems can be run on such a stand-alone workstation/storage disk combination, for optimal interactive performance it is preferable to run DISDECO on a series of computers of different speeds and sizes interconnected via a high-speed communication network such as shown in Fig. 1. From the different computational platforms available in such a CAE (Computer Aided Engineering) environment the user can select the most appropriate one in order to maintain an interactive session also for cases that require extensive numerical computations.

The central part of the whole system is the "Command and Control Processor". Its function is to control and direct the activities of the system. It starts-up and winds-down the design system, processes user input through execution of modules, creates a working environment and in general is the working partner of the user.

The link from the user to the command and control processor passes through the "Man-Machine Interface". Assuming that the user employs a terminal device or workstation which supports graphics, the man-machine interface controls the input stream from the user, analyses it, checks it for

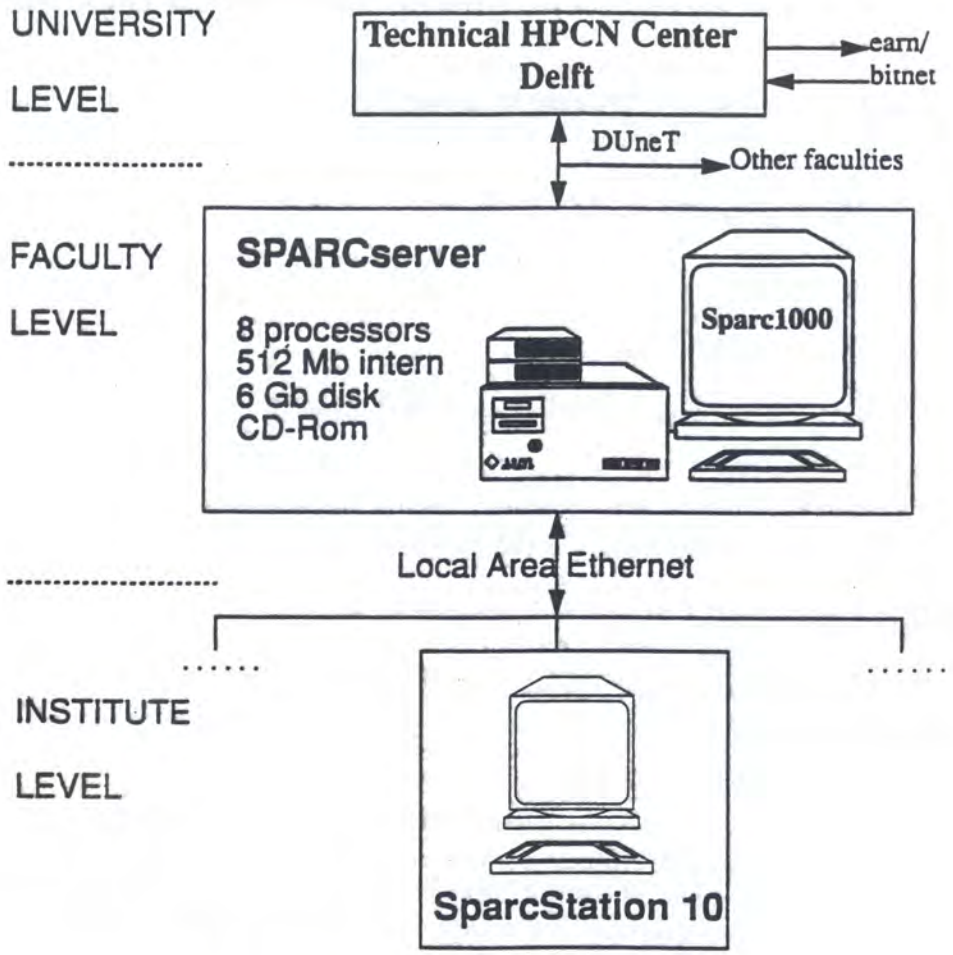

Fig. 1. Computer Aided Engineering (CAE) environment

correct syntax, validates the commands and passes it in an interpretable format to the command and control processor. In a similar manner the output stream from the design and analysis system is converted to a meaningful output for the user.

The real work of DISDECO is done by a number of dedicated "Computational Modules", arranged in a series of hierarchical levels according to the complexity of the solution processes involved.

Based on these modules the layout of DISDECO has been specifically designed so as to facilitate the search for the best nonlinear model by making it possible to study interactively the physical behavior of imperfect shell structures via models of increasing complexity.

Finally, supplementary modules provide the pre- and postprocessing functions, remote batch processing of analysis and the general utility functions needed.

3. Development of Level-1 of DISDECO

Basically the Level-1 computational modules provide the user interactively with all the information needed to make an initial estimate of the critical buckling load of a perfect cylindrical shell under the most commonly occurring external loads. Also included are modules that contain Koiter's imperfection sensitivity theory extended to anisotropic shells [5, 6]. Thus the user can immediately, in the same menu prompted interactive environment investigate the degrading effects that different types of initial imperfections may have on the critical buckling load of the perfect structure.

For all Level-1 computational modules the following Donnell type anisotropic shell equations are used

$$\mathrm{L}_A*(F) - \mathrm{L}_B*(W) = -\frac{1}{R}W_{,xx} - \frac{1}{2}\mathrm{L}_{\mathrm{NL}}(W, W + 2\bar{W})\,, \tag{1}$$

$$\mathrm{L}_B*(F) + \mathrm{L}_D*(W) = \frac{1}{R}F_{,xx} + \mathrm{L}_{\mathrm{NL}}(F, W + \bar{W}) + p\,, \tag{2}$$

where the linear operators are

$$\begin{aligned}\mathrm{L}_A*(\ ) &= A^*_{22}(\ )_{,xxxx} - 2A^*_{26}(\ )_{,xxxy} \\ &\quad + (2A^*_{12} + A^*_{66})(\ )_{,xxyy} - 2A^*_{16}(\ )_{,xyyy} + A^*_{11}(\ )_{,yyyy}\,,\end{aligned} \tag{3a}$$

$$\begin{aligned}\mathrm{L}_B*(\ ) &= B^*_{21}(\ )_{,xxxx} + (2B^*_{26} - B^*_{61})(\ )_{,xxxy} \\ &\quad + (B^*_{11} + B^*_{22} - 2B^*_{66})(\ )_{,xxyy} + (2B^*_{16} - B^*_{62})(\ )_{,xyyy} + B^*_{12}(\ )_{,yyyy}\,,\end{aligned} \tag{3b}$$

$$\begin{aligned}\mathrm{L}_D*(\ ) &= D^*_{11}(\ )_{,xxxx} + 4D^*_{16}(\ )_{,xxxy} \\ &\quad + 2\,(D^*_{12} + 2D^*_{66})(\ )_{,xxyy} + 4D^*_{26}(\ )_{,xyyy} + D^*_{22}(\ )_{,yyyy}\,,\end{aligned} \tag{3c}$$

and the nonlinear operator is

$$\mathrm{L}_{\mathrm{NL}}(S,T) = S_{,xx}T_{,yy} - 2S_{,xy}T_{,xy} + S_{,yy}T_{,xx}\,. \tag{3d}$$

Commas in the subscript denote repeated partial differentiation with respect to the independent variables following the comma. The stiffness parameters A^*_{11}, B^*_{11}, D^*_{11}, A^*_{12}, ... etc. are defined in Reference [6]. W is the component of displacement normal to the shell midsurface (here positive inward) and F is an Airy stress function. For notation and sign convention see Fig. 2.

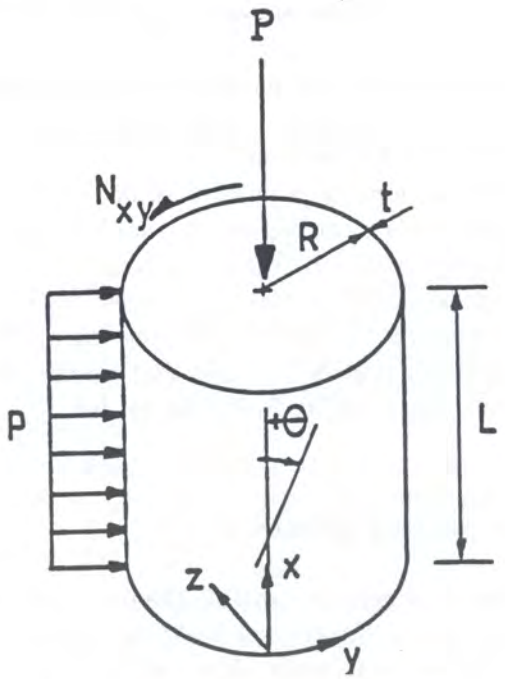

Fig. 2. Notation and sign convention

3.1. Buckling of perfect shells

By using membrane prebuckling analysis the stability problem is reduced to the solution of homogeneous partial differential equations with constant coefficients. Employing truncated double Fourier series to represent the buckling modes and the use of Galerkin type approximations then yields a standard matrix eigenvalue problem which is solved numerically. In Table 1 the capabilities of the currently operational Level-1 and Level-1$^{(+)}$ computational modules are listed.

Table 1. Level-1 and Level-1$^{(+)}$ computational modules

	Axial Compression	Internal Pressure	External Pressure	Torsion	Bending	Transverse Shear
Buckling of Perfect Shell Donnel Type Eqs. Flügge Type Eqs.	GANIBIF CYNTAPS	GANIBIF CYNTAPS	GANIBIF CYNTAPS	GANIBIF [6] CYNTAPS	BENDING [8] CYNTAPS [11]	 CYNTAPS
Axisymmetric Imperfection Donnel Type Eqs.	AXBIF	AXBIF	AXBIF	AXBIF [6]		
Asymmetric Imperfection Donnel Type Eqs.	BFACT	BFACT	BFACT	BFACT [6]		

The computational module GANIBIF is based on the buckling mode representation proposed by Khot [5]

$$W^{(1)} = t \sin m\pi \frac{x}{L} \cos \frac{n}{R}(y - \tau_{\mathrm{K}} x)\,, \tag{4}$$

where m and n are integers representing the number of axial half-waves and the number of circumferential full waves, respectively, and Khot's skewedness parameter τ_{K} [5], a real number, is introduced in order to account for the possibility of bending-twisting coupling. This module can handle combined axial compression λ_{a}, internal or external pressure $\bar{p}$ and clockwise of counterclockwise torsion $\bar{\tau}$, whereby the user must indicate which of these three basic loads he wants to use as a variable load (eigenvalue). The remaining two loads will act as fixed loads. For further details the interested reader should consult Ref. [6].

The computational module BENDING represents an extension of Seide and Weingarten's work [7] to anisotropic shells. Here the buckling mode is represented by the following truncated double Fourier-series

$$W^{(1)} = t \sin m\pi \frac{x}{L} \left\{ \sum_n C_{mn} \cos n \frac{Y}{R} \right\} + t \sin m\pi \frac{x}{L} \left\{ \sum_n D_{mn} \sin n \frac{y}{R} \right\}, \tag{5}$$

where m and n are integers representing the number of half waves and full waves in the axial and in the circumferential directions, respectively. This module can handle combined axial compression λ_{a} and bending λ_{b}, whereby the user must indicate which of the two basic loads he wants to use as a variable load (eigenvalue). The other load will act as a fixed load. For further details on this computational module see Reference [8].

It must be stressed that the Level-1$^{(+)}$ computational module CYNTAPS is based on the modified linearized Flügge type stability equations [9] extended to fully anisotropic constitutive equations. Notice that also this approach assumes a membrane prebuckling analysis. The buckling mode is represented by the following truncated double Fourier series

$$W^{(1)} = t \sum_m \sum_n C_{mn} \sin m\pi \frac{x}{L} \cos n \frac{y}{R} + \sum_m \sum_n D_{mn} \sin m\pi \frac{x}{L} \sin n \frac{y}{R}, \tag{6}$$

where m and n are integers representing the number of axial half-waves and the number of circumferential full waves, respectively. This module can handle combined axial compression λ_{a}, internal

or external pressure $\bar{p}$, clockwise or counter-clockwise torsion $\bar{\tau}$, bending λ_b and transverse shear load V. Once again the user must indicate which of the basic loads he wants to use as a variable load (eigenvalue). The remaining loads will act as fixed loads. Notice that this module represents a generalization of Meyer's [10] work to fully anisotropic shells. For further details the interested reader should consult Ref. [11].

3.2. Buckling of imperfect shells

When applying Koiter's [12] Initial Imperfection Sensitivity Theory one must differentiate between the degrading effects caused by a single mode axisymmetric imperfection or by a single mode asymmetric imperfection or by general imperfections represented by, say, a truncated double Fourier series. The currently operational Level-1 computational modules with capabilities to handle initial imperfections are listed in Table 1.

The computational module AXBIF can handle axisymmetric imperfections in the form of half-wave cosine functions

$$\bar{W} = t\bar{\xi}_1 \cos i\pi \frac{x}{L} \tag{7}$$

or half-wave sine functions

$$\bar{W} = t\bar{\xi}_1 \sin i\pi \frac{x}{L}, \tag{8}$$

where i is an integer denoting the number of half-waves in the axial direction and $\bar{\xi}_1$ is the amplitude of the axisymmetric imperfection normalized by the shell wall-thickness t. The stability problem of shells with axisymmetric imperfections is governed by a bifurcation problem with variable coefficients. Approximate solutions based on Galerkin's procedure have been obtained in the past by several authors [2, 4]. The module AXBIF represent an extension of Koiter's pioneering paper from 1963 [12] to anisotropic shells. For further details see Ref. [6].

When investigating the degrading effect of a single mode asymmetric imperfection

$$\bar{W} = t\bar{\xi}_2 \sin m\pi \frac{x}{L} \sin n\frac{y}{R}, \tag{9}$$

where m and n are integers denoting the number of axial half-waves and the number of circumferential full waves, respectively, instability occurs at the limit point of the prebuckling state in the load-deformation space as depicted in Fig. 3. The shape of the load-deflection curve for $\bar{\xi}_2 \neq 0$

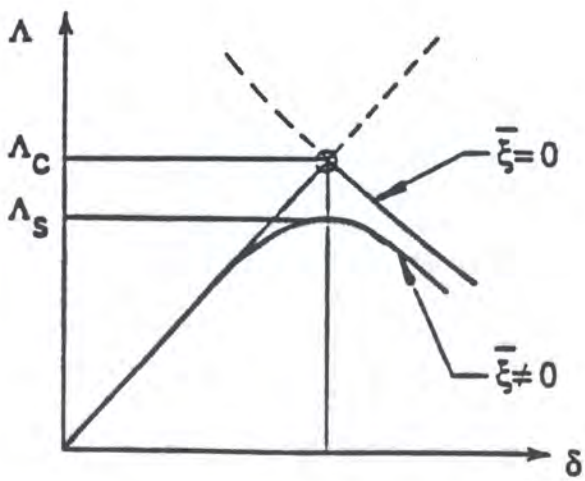

Fig. 3. Equilibrium paths of perfect and imperfect systems

can be obtained either by solving the full nonlinear response problem or by employing the well known Lyapunov–Schmidt–Koiter reduction [2, 3] technique.

Assuming that the eigenvalue problem for the critical (lowest) buckling load Λ_c will yield a unique asymmetric buckling mode $W^{(1)}$, then for imperfect shells the variation of $\Lambda(\xi\bar{\xi}_2)$ in the vicinity of the bifurcation point $\Lambda = \Lambda_c$ is given by the following asymptotic expansion [13]

$$(\Lambda - \Lambda_c)\xi = \Lambda_c\, a\xi^2 + \Lambda_c\, b\xi^3 = \dots$$

$$-\Lambda_c\, \alpha\bar{\xi}_2 - (\Lambda - \Lambda_c)\beta\bar{\xi}_2 = O(\xi\bar{\xi}_2)\,. \tag{10}$$

Expressions for the postbuckling coefficients a and b and the imperfection form factors α and β are derived in References [3, 4, 13, 14], whereby for the field-functions involved the following asymptotic expansions are used

$$W = W^{(0)}(\Lambda) + \xi W^{(1)} + \xi^2 W^{(2)} + \dots\,, \tag{11a}$$

$$F = F^{(0)}(\Lambda) + \xi F^{(1)} + \xi^2 F^{(2)} + \dots\,. \tag{11b}$$

It is customary to normalize $W^{(1)}$ with respect to the shell wall-thickness t. Notice further that $W^{(2)}$ is assumed orthogonal to $W^{(1)}$ in some appropriate sense [3, 15]. If the limit point is close enough to the bifurcation point then Λ_s, the maximum load that the structure can carry prior to buckling, can also be evaluated from Eq. (10) by maximizing Λ with respect to ξ. For cases where the first postbuckling coefficient a is identically equal to zero this yields the modified Koiter Formula [13]

$$(1 - \rho_s)^{3/2} = \frac{3}{2}\sqrt{-3\alpha^2 b}\left[1 - \frac{\beta}{\alpha}(1 - \rho_s)\right]|\bar{\xi}_2|\,, \tag{12}$$

where $\rho_s = \Lambda_s/\Lambda_c$. It should be emphasized that in all cases presented, $\bar{\xi}_2$ is normalized with respect to the shell wall-thickness and not some effective stiffness of the stiffener-shell wall combination. The computational module BFACT represents an extension of the paper by Hutchinson and Amazigo [4] to anisotropic shells following closely the work presented in Ref. [5]. For more details the interested reader should consult Ref. [6].

4. Development of Level-2 of DISDECO

All Level-2 computational modules employ a truncated Fourier expansion in the circumferential direction to eliminate the y-dependence and solve the resulting set of ordinary differential equations numerically. This makes it possible to satisfy the specified boundary conditions rigorously. See Table 2 for a listing of the capabilities of the currently operational Level-2$^{(-)}$ and Level-2 computational modules.

Table 2. Level-2$^{(-)}$ and Level-2 computational modules

	Axial Compression	Internal Pressure	External Pressure	Torsion	Bending	Transverse Shear
Buckling of Perfect Shell						
Donnel Type Eqs.	ANILISA	ANILISA	ANILISA	ANILISA [19]		
Flügge Type Eqs.	STACY	STACY	STACY	STACY	STACY [16]	STACY
Novozhilov Type Eqs.	ANOVSI	ANOVSI	ANOVSI	ANOVSI		
Axisymmetric Imperfection						
Donnel Type Eqs.	COLLAPSE	COLLAPSE	COLLAPSE	COLLAPSE [17]		
Asymmetric Imperfection						
Donnel Type Eqs.	ANILISA	ANILISA	ANILISA	ANILISA [19]		
Novozhilov Type Eqs.	ANOVSI	ANOVSI	ANOVSI	ANOVSI [22]		

4.1. Buckling of perfect shells

With the Level-2$^{(-)}$ program STACY [16] one can calculate the buckling load of anisotropic shells under combined axial compression λ_a, internal of external pressure $\bar{p}$, clockwise of counter-clockwise torsion $\bar{\tau}$, bending λ_b and transverse shear load V. The user must designate one of the basic loads as the variable load (eigenvalue). The remaining loads will act as fixed loads. This module solves the modified Flügge type linearized stability equations (9). It is based on a membrane prebuckling analysis and the specified boundary conditions of the buckling problem are rigorously satisfied. See Ref. [16] for further details.

4.2. Buckling of imperfect shells

The currently operational Level-2 computational modules with capabilities to handle initial imperfections are listed in Table 2. The computational module COLLAPSE [17] can handle axisymmetric initial imperfections given by Eqs. (7) or (8) by solving a response problem with a small axisymmetric and a vanishingly small asymmetric imperfection. It has been shown in Ref. [18] that the 2 separate branches of the response curve clearly define the location of the bifurcation point, if the successive eigenvalues are not closely spaced. For nearly simultaneous eigenvalues this approach may fail because of nonlinear modal interaction.

To investigate the degrading effect of a single asymmetric imperfection given by Eq. (9) one can use the Level-2 computational module ANILISA [19], if the critical buckling load (the lowest eigenvalue) is single valued with an asymmetric buckling mode

$$W^{(1)} = t\left[w_1(x)\cos n\frac{y}{R} + w_2(x)\sin n\frac{y}{R}\right]. \tag{13}$$

ANILISA uses the Donnell type anisotropic shell equations, employs either membrane or a nonlinear prebuckling analysis and can handle combined axial compression λ_a, internal or external pressure $\bar{p}$ and clockwise or counter-clockwise torsion $\bar{\tau}$. The specified boundary conditions are rigorously satisfied.

If the critical buckling load (the lowest eigenvalue) is multi-valued, that is, there exist (nearly) simultaneous buckling modes, then one must modify the perturbation expansions given by Eqs. (10) and (11) appropriately to read

$$(\Lambda - \Lambda_c^I) = \Lambda_c^I\, a_{ij}^I \xi_i\xi_j + \Lambda_c^I\, b_{ijk}^I \xi_i\xi_j\xi_k + \dots$$

$$-\Lambda_c^I\, \alpha_i^I \bar{\xi}_i - (\Lambda - \Lambda_c^I)\beta_i^I \bar{\xi}_i + \mathrm{O}(\xi_i\bar{\xi}_j), \quad I = 1, 2, \dots, N, \tag{14}$$

where N is the number of (nearly) simultaneous modes, repeated lower indices imply summation but repeated upper case indices I imply no summation. Expressions for the post-buckling coefficients a_i^I, b_{ijk}^I and for the imperfection form factors α_i^I, β_i^I are derived in Ref. [20] using membrane prebuckling and in Ref. [21] for nonlinear prebuckling, whereby for the field-functions involved the following asymptotic expansions are used

$$W = W^{(0)}(\Lambda) + \xi_i W_i^{(1)} + \xi_i\xi_j W_{ij}^2 + \dots, \quad i, j = 1, 2, \dots, N, \tag{15a}$$

$$F = F^{(0)}(\Lambda) + \xi_i F_i^{(1)} + \xi_i\xi_j F_{ij}^2 + \dots, \quad i, j = 1, 2, \dots, N. \tag{15b}$$

The computational module ANOVSI [22] solves Novozhilov type anisotropic shell equations, it uses either membrane or nonlinear prebuckling analysis, satisfies the specified boundary conditions rigorously and can handle combined axial compression, internal or external pressure and torsion. Once again one of the basic loads must be chosen as the variable load (eigenvalue) while the remaining two loads act as fixed loads. For further details consult Ref. [22].

5. Development of Level-3 of DISDECO

At this stage there are no plans to develop new 2-dimensional computational modules based on finite difference or finite element approach. It is felt that the highest level of complexity can be provided by any of the currently available 2-dimensional codes with advanced capabilities to handle geometric and material nonlinearities. The chosen routine can be brought via interfaces within the interactive, menu-prompted environment of DISDECO. Thus it is possible to use the same pre- and postprocessing routines at all 3 levels of computational complexity. At present different members of the STAGS family [23, 24] are being used as Level-3 computational modules.

6. Numerical results

Thanks to extensive NASA sponsored research programs carried out in the sixties and in the early seventies, the degrading effect of initial geometric imperfections has been extensively investigated using Koiter's general postbuckling theory [2, 3, 4]. Though it was found that besides boundary conditions [25] and nonlinear modal interaction [20] also the use of a rigorous prebuckling analysis [26, 27] can affect the predicted imperfection sensitivity of the buckling loads, it is customary to rely on membrane prebuckling analysis for the initial computations.

Thus with the Level-1 computational modules of DISDECO, described in Reference [6], all computations are carried out assuming a membrane prebuckling state. The accuracy of these predictions can then be verified by Level-2 computational modules such as ANILISA [19] or ANOVSI [22], which include both a rigorous prebuckling analysis and a rigorous satisfaction of the prescribed boundary conditions.

6.1. Stringer stiffened shell AS-2

The stringer stiffened shell AS-2 was cut from 6061-T6 aluminium alloy seamless tubing. The inside was first machined to the proper diameter and then the tube was placed on a steel mandrel by heating the aluminium to about 40° C. The outside stringers were cut by using an indexing head with a milling machine. The geometric and material properties of shell AS-2 are listed in Table 3. This shell was part of a series of tests carried out in a controlled end-displacement type testing machine. All tests were preceded by a complete imperfection survey [28] of the test specimen. For a detailed description of the test program see Reference [29]. All test specimens were designed for overall instability, which can also be seen on the post-buckling patterns displayed in Fig. 4.

Table 3. Geometric properties of the stringer stiffened shell AS-2 [28]

t	=	$1.96596 \cdot 10^{-2}$	cm	$(= 0.00774$	in	$)$
L	=	13.970	cm	$(= 5.50$	in	$)$
R	=	10.160	cm	$(= 4.00$	in	$)$
d_1	=	$8.03402 \cdot 10^{-1}$	cm	$(= 0.3163$	in	$)$
e_1	=	$-3.36804 \cdot 10^{-2}$	cm	$(= -0.01326$	in	$)$
A_1	=	$7.98708 \cdot 10^{-3}$	cm^2	$(= 0.1238 \cdot 10^{-2}$	in^2	$)$
I_{11}	=	$1.50384 \cdot 10^{-6}$	cm^4	$(= 0.3613 \cdot 10^{-7}$	in^4	$)$
I_{t1}	=	$4.94483 \cdot 10^{-6}$	cm^4	$(= 0.1188 \cdot 10^{-6}$	in^4	$)$
I_{t1}	=	$6.89472 \cdot 10^{6}$	N/cm^2	$(= 10 \cdot 10^{6}$	psi	$)$
ν	=	0.3				

The results of buckling load calculations with the different computational modules are summarized in Table 4. Notice that all results are given in normalized form, with the factor used for

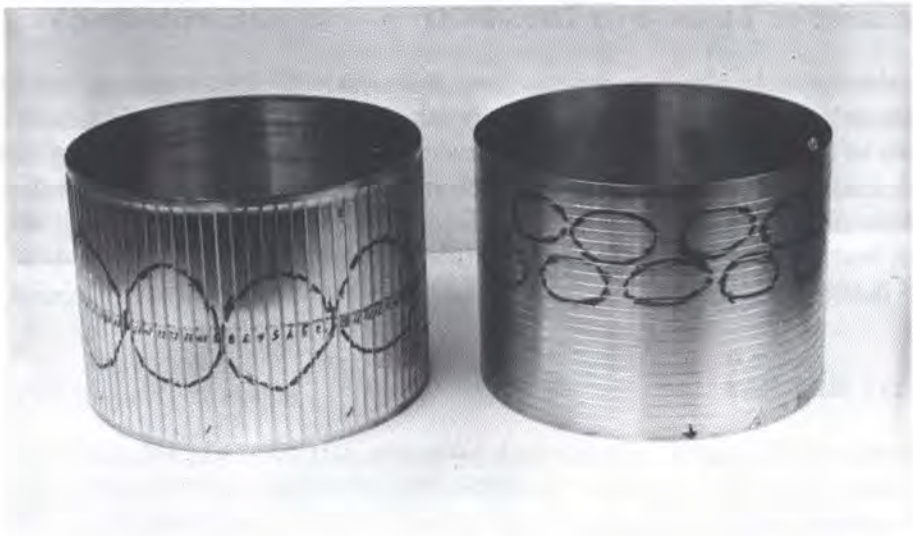

Fig. 4. Postbuckling patters for ring- and stringer stiffened shells [28]

normalization $N_{\rm cl} = -90.644$ lb/in printed in the heading of the table. Hence the critical buckling loads can be calculated directly via a simple multiplication.

Thus the Level-1 module GANIBIF [6], which uses membrane prebuckling analysis, predicts a critical buckling load of $N_{\rm c}^{\rm m} = 1.44316(-90.644) = -130.814$ lb/in, whereas if one employs the Level-2 module ANILISA [19], which uses nonlinear prebuckling analysis and satisfies the SS-3 boundary conditions ($N_x = v = W = M_x = 0$) rigorously, one obtains a critical buckling load of $N_{\rm c}^{\rm nl} = 1.42990(-90.644) = -129.612$ lb/in. In both cases buckling occurs with $n = 10$ full waves in the circumferential direction.

The explanation for this rather good agreement becomes obvious if one considers the corresponding mode shapes displayed in Fig. 5. Notice that the prebuckling deformation can reasonably well be approximated by a constant radial displacement, as is done when one uses a membrane prebuckling analysis, if the edge effects are neglected. Further, the buckling mode resembles very closely the half wave sine dependence in the axial direction used in the simplified Level-1 type analysis incorporated in GANIBIF. For better illustration the postbuckling modes w_α and w_β, which are needed for the evaluation of the second postbuckling coefficient b and the imperfection form factors α and β, are displayed normalized to one using as divisor their maximum amplitudes indicated in the figure.

When investigating the imperfection sensitivity of the critical buckling loads based on Koiter's formula Eq. (12), two different imperfection models are employed. The first one is in the form of (affine to) the lowest buckling mode

$$\bar{W} = t\bar{\xi}_2\, w_1(x)\, \cos n\theta\,, \tag{16a}$$

whereas the second is represented by a trigonometric expression

$$\bar{W} = t\bar{\xi}_2\, \sin \pi \frac{x}{L}\, \cos n\theta\,. \tag{16b}$$

From the numerical results obtained for an imperfection amplitude of $\bar{\xi}_2 = 1.0$ (one wall-thickness, thus), one sees that there is not much difference between the collapse loads predicted by the two imperfection models. The explanation is obvious, since according to Fig. 5b the form of $w_1(x)$ is practically identical to a half wave sine function. Notice that once again all results are given in normalized form. Hence the critical collapse loads can be calculated directly by simple multiplications. Thus, for instance, ANILISA predicts that if an asymmetric imperfection with the shape of the critical buckling mode and with an amplitude equal to one wall thickness is present, the maximum

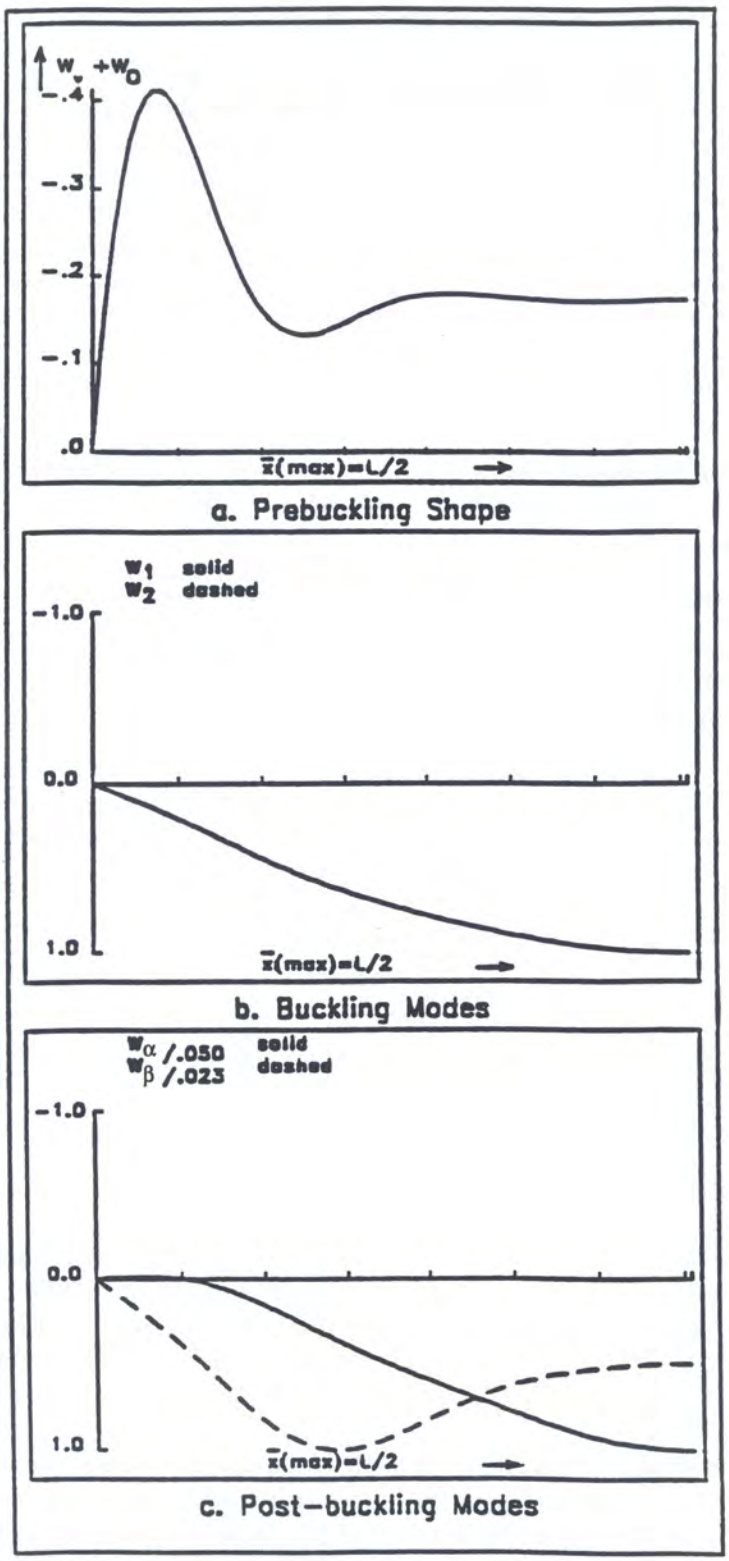

Fig. 5. Mode shapes of the axially compressed stringer stiffened shell AS-2 (Nonlinear prebuckling, $N_x = v = W = M_x = 0$ [30])

load the stringer stiffened shell AS-2 can carry is

$$N_s = \lambda_s N_{cl} = (0.603\lambda_c^{nl})N_{cl} = 0.603(1.42990)(-90.644) = -78.156 \text{ lb/in}.$$

Before a collapse analysis using the Level-3 computational model STAGS-A [23] with the assumed imperfections can be carried out, it is necessary to perform the appropriate convergence studies [31]. Initially since $n = 10$ it was decided to model only 1/20 of the circumference of the shell ($\Delta\theta = 18°$) and half of the shell length. Thus at $\theta = 0$, $\theta = 18$ and $x = 2.75$ symmetry conditions can be used. In the convergence study both the number of mesh points in the axial and in the circumferential direction must be varied. As is known, in STAGS-A the convergence is for increasing number of mesh points from above for the axial direction and from below for the circumferential direction. The results listed in Table 4 are for a mesh of 41×41, which yields critical buckling loads accurate to within less than 0.5%. As can be seen from Fig. 6 the mode shapes calculated with STAGS-A for bifurcation buckling using nonlinear prebuckling agree closely with those of Fig. 5 obtained with ANILISA [19].

Table 4. Summary of results — Axially compressed stringer stiffened shell AS-2
($N_{cl} = -90.644$ lb/in — B.C.: $N_x = v = W = M_x = 0$)

Code	Buckling load	Imperfection sensitivity $\bar{\xi}_2 = 1.0$			
		$\bar{W} = t\bar{\xi}_2 w_1(x)\cos n\theta$		$\bar{W} = t\bar{\xi}_2 \sin(\pi x/L)\cos n\theta$	
GANIBIF [6]	$\lambda_c^m = 1.44316$ (n=10)			$b = -0.03081$ $\alpha = 1.0$ $\beta = 1.0$	$\rho_s = \frac{\lambda_s}{\lambda_c^{nl}} = 0.585$
ANILISA [19]	$\lambda_c^{nl} = 1.42990$ (n=10)	$b = -0.02868$ $\alpha = 0.94093$ $\beta = 0.93948$	$\rho_s = \frac{\lambda_s}{\lambda_c^{nl}} = 0.603$	$b = -0.02868$ $\alpha = 0.92184$ $\beta = 0.91020$	$\rho_s = \frac{\lambda_s}{\lambda_c^{nl}} = 0.606$
ANOVSI [21]	$\lambda_c^{nl} = 1.41637$ (n=10)	$b = -0.02998$ $\alpha = 0.94388$ $\beta = 0.94201$	$\rho_s = \frac{\lambda_s}{\lambda_c^{nl}} = 0.603$		
STAGS [23]	$\lambda_c^{nl} = 1.40708$ (n=10)		$\rho_s = \frac{\lambda_s}{\lambda_c^{nl}} = 0.582$		$\rho_s = \frac{\lambda_s}{\lambda_c^{nl}} = 0.522$

6.2. Ring stiffened shell AR-1

The ring stiffened shell AR-1 was cut from 6061-T6 aluminium alloy tubing by the same procedure as described earlier for the stringer stiffened shell AS-2 with the only difference that the outside rings were cut on a lathe. The geometric and material properties of the shell AR-1 are listed in Table 5. This shell was part of the same test serie [29] as the shell AS-2 and as such a complete imperfection survey of shell AR-1 is available [28]. It failed in overall instability and its postbuckling pattern is shown in Fig. 4.

The results of buckling load calculations with the different computational modules are summarized in Table 6. All results are given in normalized form. The factor used for normalization $N_{cl} = -130.585$ lb/in is printed in the heading of the table. Notice that in this case the Level-1 module GANIBIF [6], which uses membrane prebuckling analysis, predicts a critical buckling load of $N_c^m = 1.09938(-130.585) = -143.563$ lb/in with a short wave ($i = 17$ [30]) axisymmetric ($n = 0$) buckling mode. Remember, this implies that for this case Koiter's b-factor method cannot be used to investigate the effect of asymmetric imperfections [4, 6]. However, from previous experience [29, 30] one expects that the use of more refined analyses will yield quite a different buckling mode. Indeed

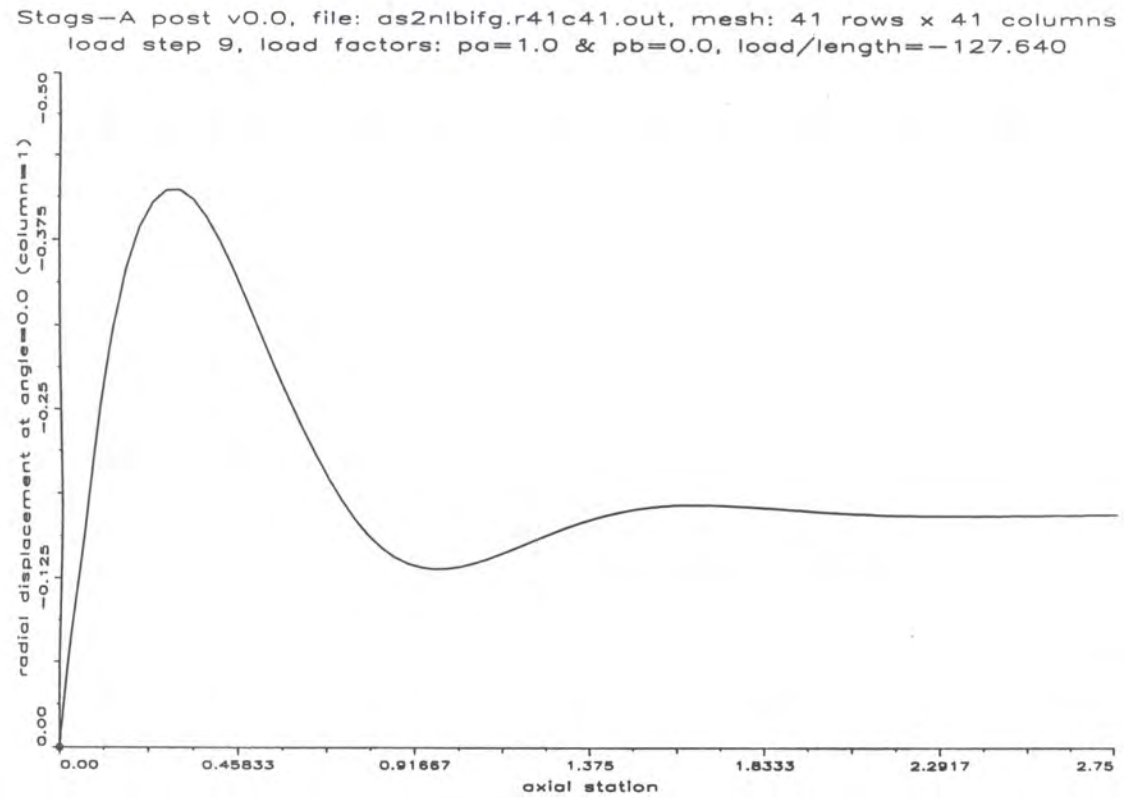

a) Prebuckling shape

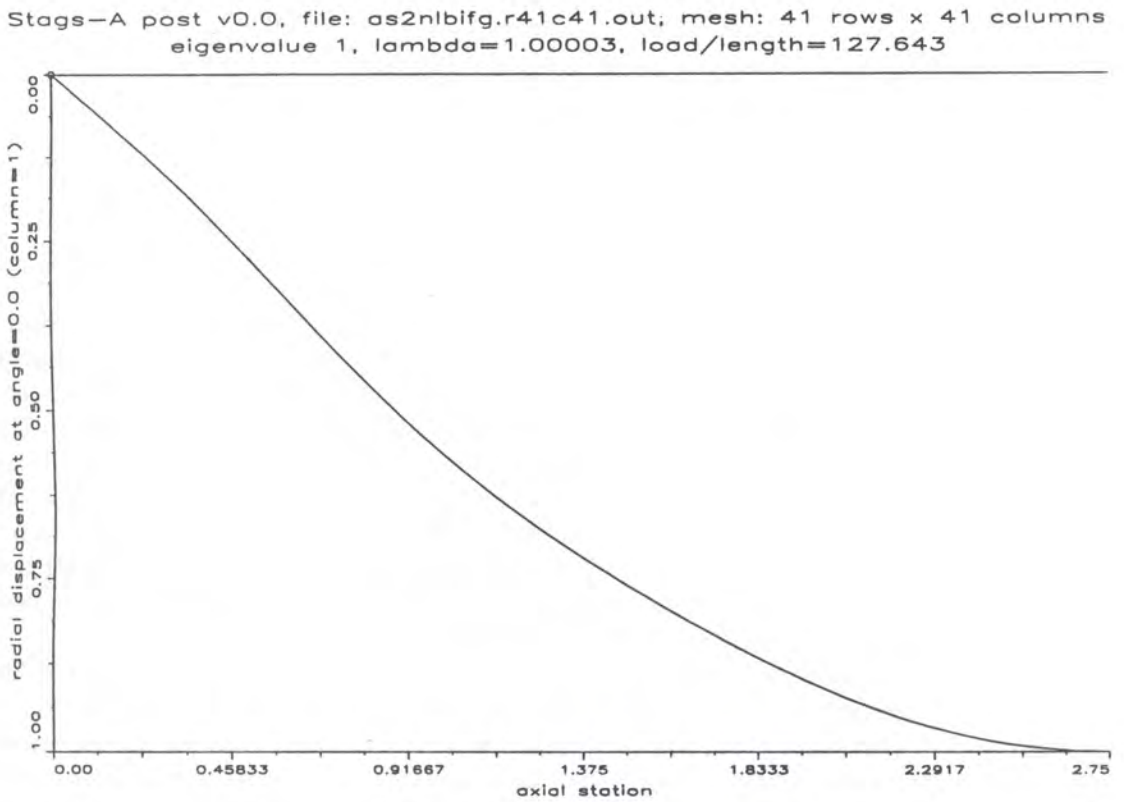

b) Buckling shape

Fig. 6. Mode shapes of the axially compressed stringer stiffened shell AS-2
(Nonlinear prebuckling, $N_x = v = W = M_x = 0$, STAGS-A [23] run)

Table 5. Geometric properties of the ring stiffened shell AR-1 [28]

t	=	$2.35966 \cdot 10^{-2}$	cm	$(= 0.00929$	in	$)$
L	=	13.335	cm	$(= 5.25$	in	$)$
R	=	10.160	cm	$(= 4.00$	in	$)$
d_2	=	0.635	cm	$(= 0.25$	in	$)$
e_2	=	$-2.66192 \cdot 10^{-2}$	cm	$(= -0.01048$	in	$)$
A_2	=	$3.06403 \cdot 10^{-3}$	cm^2	$(= 4.74925 \cdot 10^{-4}$	in^2	$)$
I_{22}	=	$2.40286 \cdot 10^{-7}$	cm^4	$(= 5.77289 \cdot 10^{-9}$	in^4	$)$
I_{t2}	=	$7.75651 \cdot 10^{-7}$	cm^4	$(= 1.86351 \cdot 10^{-8}$	in^4	$)$
I_{t1}	=	$6.89472 \cdot 10^{6}$	N/cm^2	$(= 10 \cdot 10^{6}$	psi	$)$
ν	=	0.3				

Table 6. Summary of results — Axially compressed ring stiffened shell AR-1 ($N_{cl} = -130.585$ lb/in — B.C.: $N_x = v = W = M_x = 0$)

Code	Buckling load	Imperfection sensitivity $\bar{\xi}_2 = 1.0$			
		$\bar{W} = t\bar{\xi}_2 w_1(x) \cos n\theta$		$\bar{W} = t\bar{\xi}_2 \sin(\pi x/L) \cos n\theta$	
GANIBIF [6]	$\lambda_c^m = 1.09938$ (n=0)				
ANILISA [19]	$\lambda_c^{nl} = 1.01444$ (n=14)	$b = -0.23172$ $\alpha = 0.24104$ $\beta = 0.56706$	$\rho_s = \frac{\lambda_s}{\lambda_c^{nl}} = -0.013$	$b = -0.23172$ $\alpha = 0.01085$ $\beta = 0.02042$	$\rho_s = \frac{\lambda_s}{\lambda_c^{nl}} = 0.947$
ANOVSI [21]	$\lambda_c^{nl} = 1.01400$ (n=14)	$b = -0.23015$ $\alpha = 0.024264$ $\beta = -0.56570$	$\rho_s = \frac{\lambda_s}{\lambda_c^{nl}} = -0.0094$		
STAGS [23]	$\lambda_c^{nl} = 1.01516$ (n=14)		$\rho_s = \frac{\lambda_s}{\lambda_c^{nl}} = 0.596$		$\rho_s = \frac{\lambda_s}{\lambda_c^{nl}} = 0.792$

with the Level-2 module ANILISA [19], which uses nonlinear prebuckling analysis and satisfies the SS-3 boundary conditions ($N_x = v = W = M_x = 0$) rigorously, one obtains a critical buckling load of $N_c^{nl} = 1.01444(-130.585) = -132.471$ lb/in with $n = 14$ full waves in the circumferential direction, an asymmetric buckling mode thus. Looking at the mode shapes depicted in Fig. 7, one sees that the prebuckling mode consists of a sinusoidal pattern with 17 half waves in the axial direction, which however has a strong attenuation away from the shell edges. The buckling mode displays a very accentuated edge buckling type behavior, whereby significant displacements occur only close to the shell edges. Notice that also the postbuckling modes w_α and w_β, which for better illustration are depicted normalized to one using as divisor their maximum amplitudes indicated in the figure, display large displacements close to the shell edges.

To investigate the imperfection sensitivity of the critical (asymmetric) buckling load Koiter's formula given by Eq. (12) is used. Hereby the previously mentioned two distinct imperfection models specified by Eqs. (16a) and (16b) are employed. Obviously the fact that for an imperfection shape affine to (similar to) the buckling mode with an amplitude of $\bar{\xi}_2 = 1.0$ one obtains a negative load carrying capacity is unrealistic. Here one must remember that Koiter's Imperfection Sensitivity Theory is asymptotically exact, that is, it yields accurate predictions for sufficiently small imperfections, whereby what is sufficiently small may vary from case to case. Also Eq. (12) was obtained by maximizing the perturbation expansion given by Eq. (10), where terms of $O(\xi, \bar{\xi})$ are

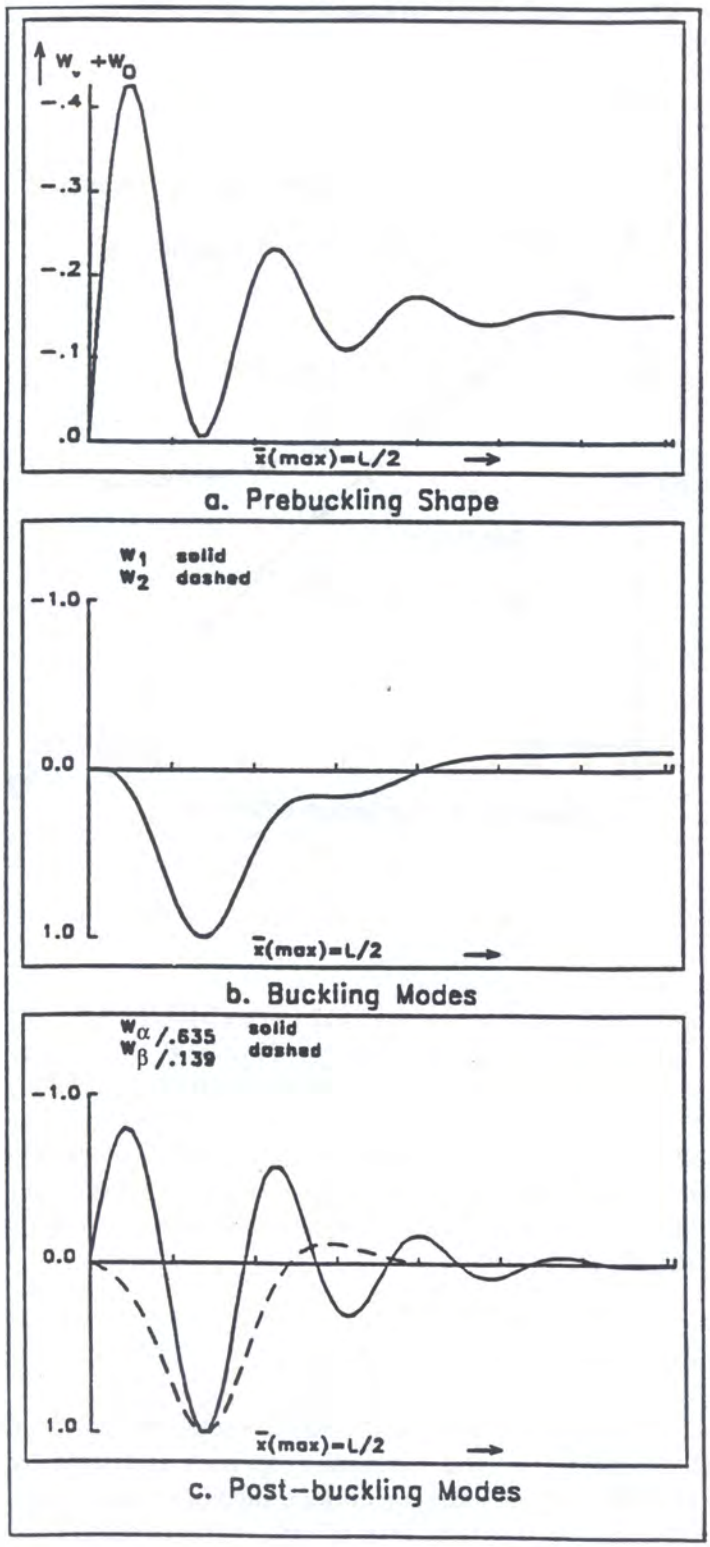

Fig. 7. Mode shapes of the axially compressed ring stiffened shell AR-1 (Nonlinear prebuckling, $N_x = v = W = M_x = 0$ [30]

neglected. As can be seen from the results plotted in Fig. 8 by using more advanced computational modules such as COLLAPSE [17], where nonlinear terms up to order $(\xi, \bar{\xi})$ are kept, one obtains more reasonable predictions.

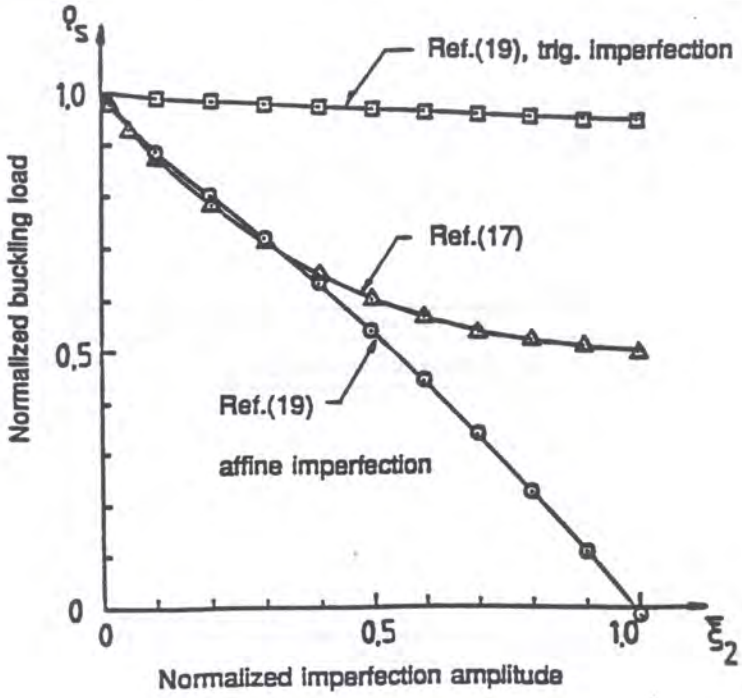

Fig. 8. Imperfection sensitivity of the ring stiffened shell AR-1 for asymmetric imperfections (Axial compression)

Since $n = 14$ for the STAGS-runs it was decided to model only 1/28 of the circumference of the shell ($\Delta\theta = 12.8571°$) and half of the shell length. Thus at $\theta = 0$, $\theta = 12.8571$ and $x = 2.625$ symmetry conditions can be used. The convergence study resulted in a mesh of 321×41 in order to yield critical buckling loads accurate to within 0.5%. As can be seen from Fig. 9 the modes shapes calculated with STAGS-A for bifurcation buckling using nonlinear prebuckling agree closely with those of Fig. 7 obtained with ANILISA [19]. Notice also that the STAGS-run with an asymmetric imperfection affine to (similar to) the critical buckling mode confirms the prediction obtained by the Level-2 module COLLAPSE [17].

6.3. Khot's glass-epoxy shell (–40°, 40°, 0°)

As a last example one of the glass-epoxy shells first presented by Khot and Venkayya in their 1970 paper [5] is used. Its geometric and material properties are listed in Table 7. Due to an unsymmetrical lay-up of (–40°, 40°, 0°) the membrane, membrane-bending coupling and bending stiffness matrices A_{ij}, B_{ij} and D_{ij} are full. This can make the nonlinear coupling effect between adjacent buckling modes become significant.

The results of buckling load calculations with the different computational modules are summarized in Table 8. Notice that all results are presented in normalized form, with the factor used for normalization $N_{\mathrm{cl}} = -965.9814$ lb/in listed in the heading of the table. In this case the Level-1 module GANIBIF [6], which uses membrane prebuckling analysis, predicts a critical buckling load of $N_{\mathrm{c}}^{\mathrm{m}} = 0.540706\ (-965.9814) = -522.312$ lb/in with a skewed buckling pattern ($\tau_{\mathrm{K}} = -0.76$)

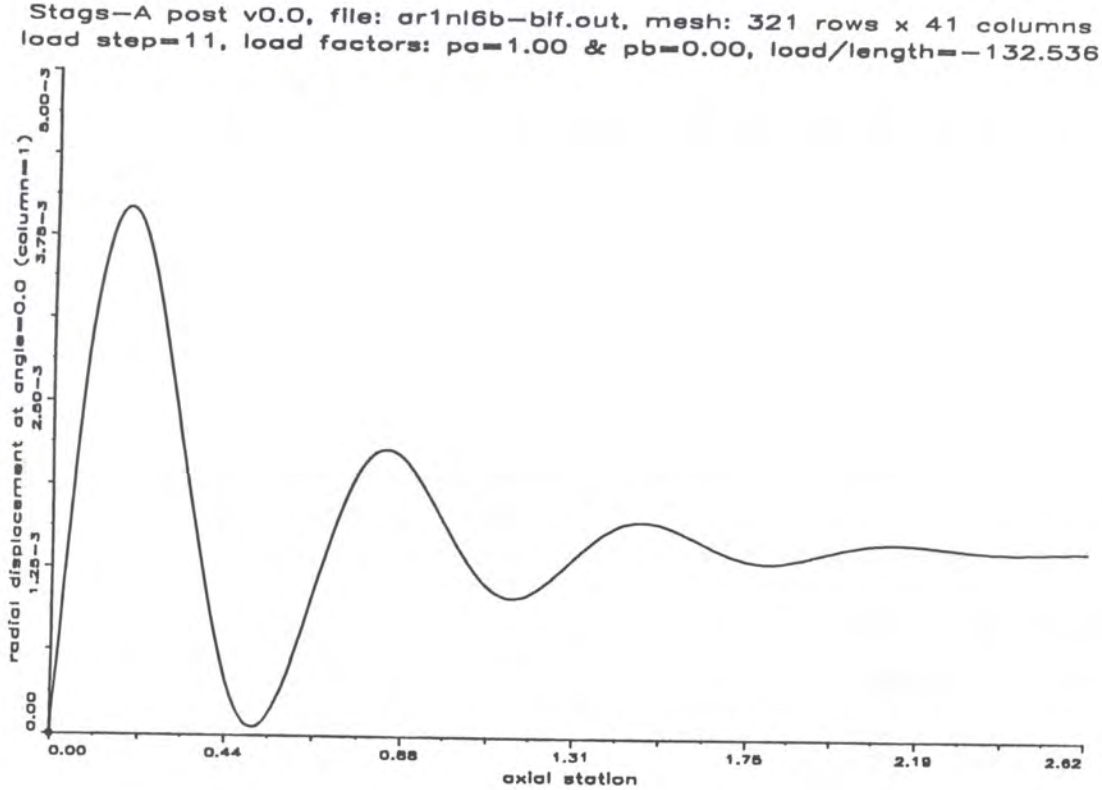

a) Prebuckling shape

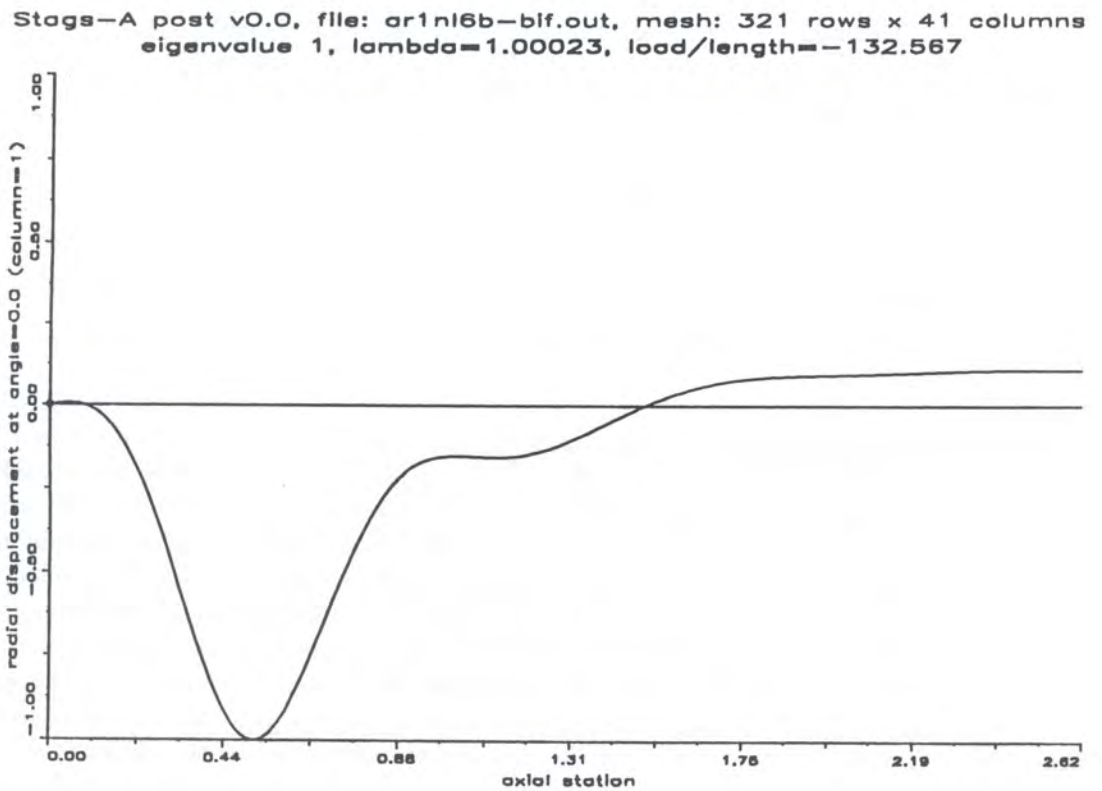

b) Buckling shape

Fig. 9. Mode shapes of the axially compressed ring stiffened shell AR-1
(Nonlinear prebuckling, $N_x = v = W = M_x = 0$, STAGS-A [23] run)

Table 7. Geometric properties of Khot's [5] glass-epoxy shells

t_{total}	=	$9.14400 \cdot 10^{-2}$	cm	(= 0.036	in)
L	=	31.750	cm	(= 12.5	in)
R	=	15.240	cm	(= 6.00	in)
E_{11}	=	$5.17104 \cdot 10^{6}$	N/cm^2	$(= 7.5 \cdot 10^{6}$	psi)
E_{22}	=	$2.41315 \cdot 10^{6}$	N/cm^2	$(= 3.5 \cdot 10^{6}$	psi)
G	=	$8.61840 \cdot 10^{5}$	N/cm^2	$(= 1.25 \cdot 10^{6}$	psi)
ν_{12}	=	0.25			

Note:

$\nu_{21} = \nu_{12} E_{22}/E_{11}$

Cylindrical shells with 3 layers of equal thicknesses (= 0.012 in)

Table 8. Summary of results — Axially compressed Khot's glass-epoxy shell $(-40°, 40°, 0°)$ ($N_{\text{cl}} = -965.9814$ lb/in — B.C.: $N_x = v = W = M_x = 0$)

Code	Buckling load	Imperfection sensitivity $\bar{\xi}_2 = 1.0$			
		$\bar{W} = t\bar{\xi}_2[w_1(x)\cos n\theta + w_2(x)\sin n\theta]$		$\bar{W} = t\bar{\xi}_2 \sin(\pi x/L)\cos n\theta$	
GANIBIF [6]	$\lambda_c^{\text{m}} = 0.540706$ (n=12) at $\tau_{\text{K}} = -0.76$			$b = -0.015958$ $\alpha = 1.0$ $\beta = 1.0$	$\rho_{\text{s}} = \frac{\lambda_{\text{s}}}{\lambda_c^{\text{nl}}} = 0.644$
ANILISA [19]	$\lambda_c^{\text{nl}} = 0.536362$ (n=12)	$b = -0.38935$ $\alpha = 0.89751$ $\beta = 0.66444$	$\rho_{\text{s}} = \frac{\lambda_{\text{s}}}{\lambda_c^{\text{nl}}} = 0.251$	$b = -0.38935$ $\alpha = 0.003702$ $\beta = 0.010209$	$\rho_{\text{s}} = \frac{\lambda_{\text{s}}}{\lambda_c^{\text{nl}}} = 0.969$
ANOVSI [21]	$\lambda_c^{\text{nl}} = 0.533222$ (n=12)	$b = -0.08963$ $\alpha = 0.90577$ $\beta = 0.69749$	$\rho_{\text{s}} = \frac{\lambda_{\text{s}}}{\lambda_c^{\text{nl}}} = 0.541$		
STAGS [23]	$\lambda_c^{\text{nl}} = 0.502623$ (n=12)		$\rho_{\text{s}} = \frac{\lambda_{\text{s}}}{\lambda_c^{\text{nl}}} = 0.749$		$\rho_{\text{s}} = \frac{\lambda_{\text{s}}}{\lambda_c^{\text{nl}}} = ?$

consisting of $n = 12$ full waves in the circumferential direction. With the Level-2 module ANILISA [19], which uses nonlinear prebuckling analysis and satisfies the SS-3 boundary conditions ($N_x = v = W_x = M = 0$) rigorously, one obtains a critical buckling load of $N_c^{\text{nl}} = 0.536362(-965.9814) = -518.116$ lb/in. From the mode shapes obtained by ANILISA and depicted in Fig. 10 one sees that once again the prebuckling shape can reasonably well be approximated by a constant radial displacement, as is done when one uses membrane prebuckling analysis, if the edge effects are neglected. Further, as has been shown in Ref. [30] the component functions $w_1(x)$ and $w_2(x)$ of the skewed buckling mode given by Eq. (13) agree well with the corresponding component functions of Khot's buckling mode given by Eq. (14). However, when one compares the shapes of the second order field functions w_α, w_β and w_γ there are significant discrepancies [30], which accounts for the large differences in the imperfection sensitivity predictions as represented by the values of $\alpha^2 b$. The fact that for anisotropic shells one cannot fully rely on the imperfection sensitivity predictions of simplified analyses based on membrane prebuckling has been also noticed earlier by Tennyson et al [27].

Another significant difference in the predicted imperfection sensitivity occurs when one switches from Donnell type equations to the more accurate Novozhilov type equations. Considering the

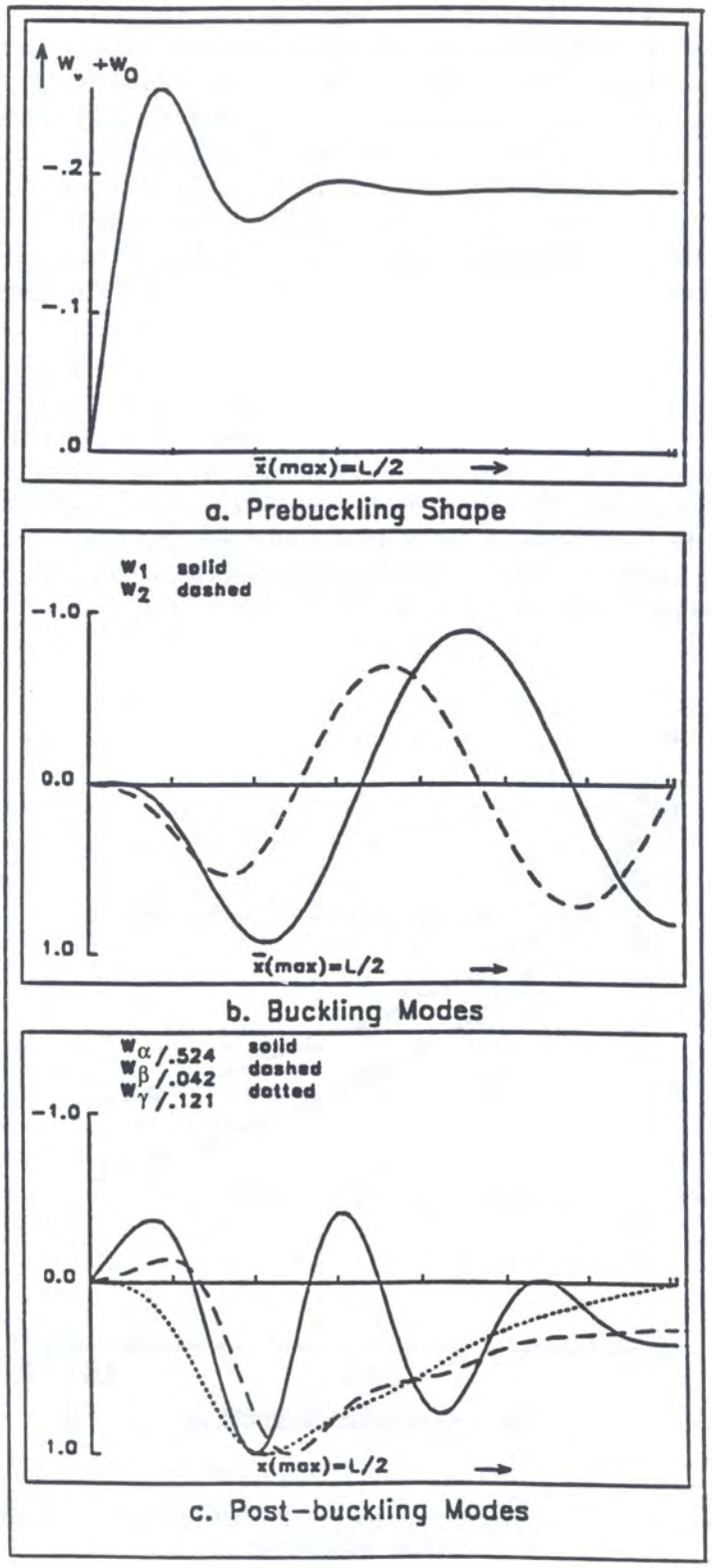

Fig. 10. Mode shapes of Khot's glass-epoxy shell $(-40°, 40°, 0°)$ under axial compression (Nonlinear prebuckling, $N_x = v = W = M_x = 0$ [30]

results listed in Table 8, one sees that whereas ANOVSI [21] predicts a critical buckling load of $N_c^{nl} = 0.533222(-965.9814) = -515.083$ lb/in, which is only about 0.6% lower than the critical buckling load predicted by ANILISA, there is a significant difference sofar as the values of the second postbuckling coefficient b are concerned. On the other hand, recall that for the stringer stiffened shell AS-2 and the ring stiffened shell AR-1 the imperfection sensitivity predictions by ANILISA and ANOVSI agreed quite well (see Tables 4 and 6). It appears that the difference for Khot's glass-epoxy shell is caused by the more accurate representation of the shearing stress resultant N_{xy} in Novozhilov type equations. Then whereas by the orthotropic shells AS-2 and AR-1 for axial compression the shearing stress resultant N_{xy} is vanishingly small, for Khot's glass-epoxy shell due to the unsymmetrical lay-up in the higher order fields the shearing stress resultant N_{xy} plays a significant role.

Still another interesting feature occurs when one investigates the imperfection sensitivity of Khot's glass-epoxy shell with ANOVSI. Due to the full stiffness matrix significant modal interaction between adjacent buckling modes occurs. Assuming that there is an asymmetric imperfection affine to (similar to) the lowest buckling mode with an amplitude of $\bar{\xi}_1$ and that there is no contribution from the adjacent buckling mode ($\bar{\xi}_2 = \xi_2 = 0$) one obtains the curve labelled "without interaction" in Fig. 11. To obtain the curve labelled "with interaction" one admits also contributions from the second lowest buckling mode ($\bar{\xi}_2 = 0$, $\xi_2 \neq 0$). This implies that one has to solve 2 equations of the form given by Eq. (14) simultaneously, whereby $\bar{\xi}_1 \neq 0$ and $\bar{\xi}_2 = 0$.

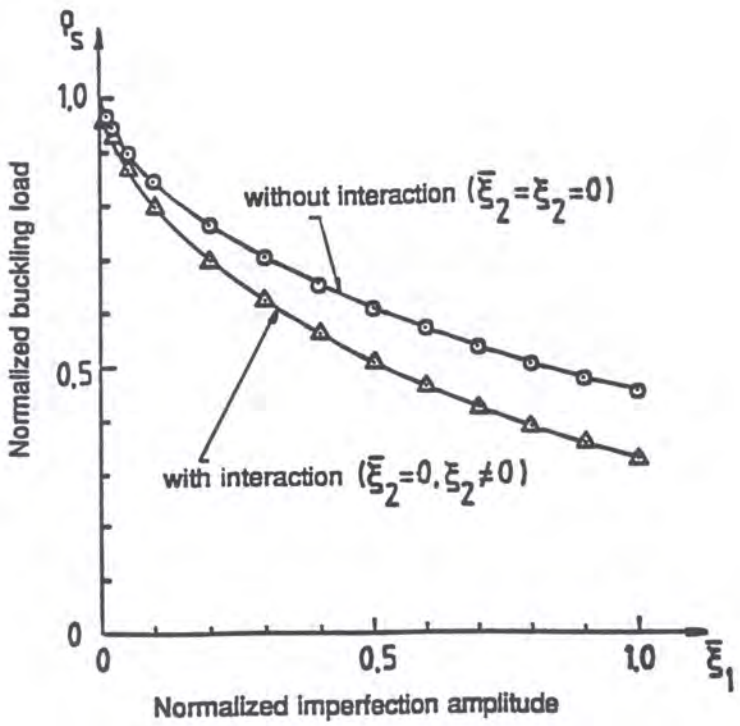

Fig. 11. Imperfection sensitivity of Khot's glass-epoxy shell (−40°, 40°, 0°) for asymmetric imperfections (Axial compression)

So far as STAGS-runs are concerned, because of the general lay-up of Khot's glass-epoxy shell and the resulting skewed buckling pattern one is forced to model the whole shell. This leads to a very large problem if one wants to maintain the accuracy of within 0.5%. Work is in progress and the results will be published in due time.

7. Conclusions

The advantages of using DISDECO's hierarchical interactive approach to shell stability analysis have been illustrated with the help of a few examples. These cases were chosen with the purpose to make it self-evident to those who follow the details of the computations, that in order to arrive at a reliable prediction of the critical buckling load and to make an estimate of its imperfection sensitivity which can be used with confidence, one must proceed step by step from simpler to more complex models and solution procedures.

In particular, one can state that for the axially compressed stringer stiffened shell AS-2, which buckles in an asymmetric mode with a single half wave in the axial direction and 10 full waves in the circumferential direction, all solution procedures work just about equally well if one uses SS-3 ($N_x = v = W = M_x = 0$) boundary conditions.

The critical buckling load of the axially compressed ring stiffened shell AR-1, on the other hand, can only be determined accurately with a Level-2 module using nonlinear prebuckling analysis. When using the discrete finite difference or finite element type Level-3 modules great care must be exercised to use a sufficiently fine mesh size in order to be able to pick up the edge-buckling type axial dependence of the asymmetric buckling mode with $n = 14$ full waves in the circumferential direction. Further it is seen that the imperfection sensitivity of the critical buckling load cannot be determined via Koiter's formula for imperfection amplitudes greater than $0.3t$. In cases where $\bar{\xi}_2 > 0.3$ one has to use more advanced computational modules which solve the nonlinear problem directly.

The last example with Khot's glass-epoxy shell demonstrates conclusively the advantages of using Level-1 and Level-2 modules for optimization purposes, leaving runs with the Level-3 module to the very end. As it turns out the critical buckling load can be determined accurately with the Level-2 modules ANILISA or ANOVSI. However, to investigate the imperfection sensitivity of the critical buckling mode one must rely on the predictions of ANOVSI, which is based on the more accurate Novozhilov type equations and takes into account the effect of nonlinear interaction between adjacent buckling modes.

Nomenclature

a, a_{ij}^I	first postbuckling coefficient
A_{ij}^*	semi-inverted extensional stiffness matrix
b, b_{ijk}	second postbuckling coefficient
B_{ij}^*	semi-inverted bending-stretching coupling matrix
c	$= \sqrt{3(1-\nu^2)}$
D_{ij}^*	semi-inverted flexural stiffness matrix
E	arbitrary chosen reference Young's modulus
F	Airy stress function
$F^{(0)}$, $F^{(1)}$, $F^{(2)}$	zeroth, first and second order fields, respectively
i	number of half waves in the axial direction
L	shell length
m	number of half waves in the axial direction
M	applied bending moment
n	number of full waves in the circumferential direction
N_a	applied compressive stress resultant
N_{xy}	applied shear stress resultant
p	external pressure
$\bar{p}$	nondimensional external pressure ($\bar{p} = (cR^2/Et^2)p$)
R	shell radius
t	shell wall-thickness

V	applied transverse shear load
$\bar{V}$	nondimensional transverse shear load parameter ($\bar{V} = (V/\pi R)(cR/Et^2)$)
w_1, w_2	buckling radial displacement functions
W	radial displacement (positive inward)
$W^{(0)}$, $W^{(1)}$, $W^{(2)}$	zeroth, first and second order fields, respectively
$\bar{W}$	initial radial imperfection ($\bar{W} = \bar{\xi}\hat{W}$)
$\hat{W}$	shape of the initial radial imperfection
x, y	axial and circumferential coordinates on the middle surface of the shell, respectively
α, α_i^I	first imperfection form factor
β, β_i^I	second imperfection form factor
θ	circumferential coordinate ($\theta = y/R$)
λ_a	nondimensional axial load parameter ($\lambda_a = (cR/Et^2)N_a$)
λ_b	nondimensional bending load parameter ($\lambda_b = (M/\pi R^2)(cR/Et^2)$)
Λ	nondimensional variable load factor
ν	arbitrary chosen reference Poisson's ratio
ξ	perturbation parameter
$\bar{\xi}_1$	amplitude of axisymmetric initial imperfection
$\bar{\xi}_2$	amplitude of asymmetric initial imperfection
ρ_s	normalized variable load factor ($\rho_s = \Lambda_s/\Lambda$)
$\bar{\tau}$	nondimensional torque parameter ($\bar{\tau} = (cR/Et^2)N_{xy}$) — positive counter-clockwise
τ_K	Khot's skewedness parameter [5]

Subscripts

$(\,)_c$	evaluated at the bifurcation point
$(\,)_s$	evaluated at the limit point

Acknowledgement

The development of DISDECO is supported in part by NASA Langley Research Center under Grant NAGW-2736. This aid and fruitful discussions with Dr. J.H. Starnes are gratefully acknowledged.

References

[1] J. Arbocz, J.M.A.M. Hol. Collapse of Axially Compressed Cylindrical Shells with Random Imperfections. *AIAA Journal*, **29**: 2247–2256, 1991.

[2] W.T. Koiter. *On the Stability of Elastic Equilibrium* (in Dutch). Ph.D. Thesis, TH-Delft, The Netherlands, H.J. Paris, Amsterdam, 1945, English translation NASA TTF-10, pp. 1–833, 1967.

[3] B. Budiansky. Post-Buckling Behavior of Cylinders in Torsion. In: F.I. Niordson, ed., *Proceedings of the Second IUTAM Symposium on Theory of Thin Shells, Copenhagen, Sept. 5–9, 1967*, 212–233. Springer Verlag Berlin-Heidelberg-New York, 1969.

[4] J.W. Hutchinson, J.C. Amazigo. Imperfection Sensitivity of Eccentrically Stiffened Cylindrical Shells. *AIAA Journal*, **5**: 392–401, 1967.

[5] N.S. Khot, V.B. Venkayya. *Effect of Fiber Orientation on Initial Postbuckling Behavior and Imperfection Sensitivity of Composite Cylindrical Shells.* Technical Report AFFDL-TR-70-125, Air Force Flight Dynamics Laboratory, Wright-Patterson Air Force Base, Ohio, December 1970.

[6] J. Arbocz. *The Effect of Initial Imperfections on Shell Stability — An Updated Review.* Report LR-695, Delft University of Technology, Faculty of Aerospace Engineering, The Netherlands, September 1992.

[7] P. Seide, V.I. Weingarten. On the Buckling of Circular Cylindrical Shells under Pure Bending. *ASME Journal of Applied Mechanics*, **28**: 112–116, 1961.

[8] A. Buitenhuis. *On the Buckling and Initial Postbuckling Behavior of Anisotropic Circular Cylindrical Shells under Combined Bending and Axial Loads.* Ir. thesis, Delft University of Technology, Faculty of Aerospace Engineering, The Netherlands, August 1992.

[9] N. Yamaki. *Elastic Stability of Circular Cylindrical Shells.* North-Holland Series in Applied Mathematics and Mechanics, Vol. 27, Elsevier-Science Publishers B.V., Amsterdam-New York-Oxford, 1984.

[10] R.R. Meyer. *Buckling of Stiffened Cylindrical Shells Subjected to Combined Axial Compression, Normal Pressure, Bending and Shear Loading.* Ph.D. Thesis, University of California at Los Angeles, 1972.

[11] H.A.J. Knops. *Buckling of Anisotropic Cylindrical Shells Subjected to Combined Axial Compression, Normal Pressure, Bending and Shear Loading.* Report LR-611, Delft University of Technology, Faculty of Aerospace Engineering, The Netherlands, December 1989.

[12] W.T. Koiter. The Effect of Axisymmetric Imperfections on the Buckling of Cylindrical Shells under Axial Compression. Koninkl. Ned. Akad. Wetenschap. Proc. B66, pp. 265–279, 1963.

[13] G.A. Cohen. Effect of a Nonlinear Prebuckling State on the Postbuckling Behavior and Imperfection Sensitivity of Elastic Structures. *AIAA Journal*, **6**: 1616–1619, 1968.

[14] J. Arbocz, J.M.A.M. Hol. *ANILISA — Computational Module for Koiter's Imperfection Sensitivity Theory.* Report LR-582, Delft University of Technology, Faculty of Aerospace Engineering, The Netherlands, January 1989.

[15] J.R. Fitch. The Buckling and Postbuckling Behavior of Spherical Caps under Concentrated Load. *Int. Journal Solids & Structures*, **4**: 421–446, 1968.

[16] E. Karyadi. *Buckling of Circular Cylindrical Shells Subjected to Combined Loads.* Memorandum M-663, Delft University of Technology, Faculty of Aerospace Engineering, The Netherlands, September 1992.

[17] J. Arbocz, R.P. Notenboom, A.J.P. van der Wekken. *COLLAPSE — Buckling of Imperfect Anisotropic Shells under Combined Loading.* Report LR-702, Delft University of Technology, Faculty of Aerospace Engineering, The Netherlands, April 1993.

[18] J. Arbocz, P.G. Vermeulen, J. van Geer. The Buckling of Axially Compressed Imperfect Shells with Elastic Edge Supports. In: I. Elishakoff et al, eds., *Buckling of Structures — Theory and Experiment, Studies in Applied Mechanics 19*, Elsevier-Science Publishers B.V., Amsterdam-New York-Oxford, 1988.

[19] J. Arbocz, J.M.A.M. Hol. Koiter's Stability Theory in a Computer Aided Engineering (CAE) Environment. *Int. J. Solids & Structures*, **26**: 945–973, 1990.

[20] E. Byskov, J.W. Hutchinson. Mode Interaction in Axially Stiffened Cylindrical Shells. *AIAA Journal*, **15**: 941–948, 1977.

[21] J. Arbocz, J. de Vries, G. Rebel. *Koiter's Stability Theory Extended to the Buckling of Anisotropic Shells with (nearly) Simultaneous Buckling Modes.* Report LR-709, Delft University of Technology, Faculty of Aerospace Engineering, The Netherlands, March 1993.

[22] G. Rebel. *ANOVSI — Computational Module for the Solution of Nonlinear Compound Eigenvalue Problems via Subspace Iteration.* Ir. Thesis, Delft University of Technology, Faculty of Aerospace Engineering, The Netherlands, March 1992.

[23] B.O. Almroth, F.A. Brogan, E. Miller, F. Zele, H.T. Peterson. *Collapse Analysis for Shells of General Shape; II. User's Manual for the STAGS — A Computer Code.* Technical Report AFFDL-TR-71-8, Air Force Flight Dynamics Laboratory, Wright-Patterson Air Force Base, Ohio, March 1973.

[24] B.O. Almroth, F.A. Brogan, G.M. Stanley. *Structural Analysis General Shells.* Lockheed Missiles and Space Co, Palo Alto, California, Vol. 2, Users Instructions for STAGSC-1, Report LMSC D633873, 1983.

[25] N.J. Hoff. Buckling of Thin Shells. In: *Proceedings of an Aerospace Symposium of Distinguished Lecturers in Honor of Theodore von Krmn on his 80th Anniversary*, 1–42. Institute of Aerospace Sciences, New York, 1961.

[26] J.W. Hutchinson, J.C. Frauenthal. Elastic Postbuckling Behavior of Stiffened and Barrelled Cylindrical Shells. *ASME Journal of Applied Mechanics*, **36**: 784–790, 1969.

[27] R.C. Tennyson, M. Booton, K.H. Chan. Buckling of Short Cylinders under Combined Loading. *ASME Journal of Applied Mechanics*, **45**: 574–578, 1978.

[28] J. Arbocz, H. Abramovitch. *The Initial Imperfection Data Bank at the Delft University of Technology — Part I.* Report LR-290, Delft University of Technology, Faculty of Aerospace Engineering, The Netherlands, December 1979.

[29] J. Singer, J. Arbocz, C.D. Babcock. Buckling of Imperfect Stiffened Cylindrical Shells under Axial Compression. *AIAA Journal*, **9**: 68–75, 1971.

[30] J. Arbocz. *Comparison of Level-1 and Level-2 Buckling and Postbuckling Solutions.* Report LR-700, Delft University of Technology, Faculty of Aerospace Engineering, The Netherlands, November 1992.

[31] J. Arbocz, C.D. Babcock Jr. *Utilization of STAGS to Determine Knockdown Factors from Measured Initial Imperfections.* Report LR-275, Delft University of Technology, Faculty of Aerospace Engineering, The Netherlands, November 1978.